Ultrasonics 56 (2015) 148–152

Contents lists available at ScienceDirect

Ultrasonics

journal homepage: www.elsevier.com/locate/ultras

Observing backfolded and unfolded acoustic phonons by broadband optical light scattering

L. Maerten [a], A. Bojahr [a], M. Bargheer [a,b,*]

[a] Institut für Physik & Astronomie, Universität Potsdam, Karl-Liebknecht-Str. 24-25, 14476 Potsdam, Germany
[b] Helmholtz-Zentrum-Berlin für Energie und Materialforschung, Wilhelm-Conrad-Röntgen Campus, BESSY II, Albert-Einstein-Str. 15, 12489 Berlin, Germany

ARTICLE INFO

Article history:
Received 20 June 2014
Received in revised form 26 August 2014
Accepted 27 August 2014
Available online 10 September 2014

Keywords:
Phonon dispersion
Phonon backfolding
Time resolved Brillouin scattering
Superlattice
Broadband detection

ABSTRACT

We use broadband time domain Brillouin scattering to observe coherently generated phonon modes in bulk and nanolayered samples. We transform the measured transients into a frequency-wavevector diagram and compare the resulting dispersion relations to calculations. The detected oscillation amplitude depends on the occupation of phonon modes induced by the pump pulse. For nanolayered samples with an appropriately large period, the whole wavevector range of the Brillouin zone becomes observable by broadband optical light scattering. The backfolded modes vanish, when the excitation has passed the nanolayers and propagates through the substrate underneath.

1. Introduction

The advent of mode locked laser systems has lead to the exciting field of picosecond ultrasonics [1]. Coherently generated phonons can be studied using this powerful technique [1–4]. In contrast to frequency domain techniques, the spectral resolution of time domain scattering is only limited by the observed temporal range. The maximum frequency that can be resolved is limited by the temporal width of the excitation and probing pulses. The observable range of phonon wavevectors is primarily determined by the probe light spectrum [5]. The fraction of the Brillouin zone that can be covered by this spectrum, however, depends on the sample structure. In a superlattice, backfolding of phonon branches at the new Brillouin zone edge occurs due to the enlarged artificial unit cell and the thus narrower Brillouin zone. This backfolding of phonons has first been studied by Colvard et al. [6] using Raman scattering techniques and later also using time resolved methods [2–4,7]. More recent studies have concentrated on shaping the excitation profile [3,8–12], designing suitable superlattices for detection [9,13,14] and building phonon [15] and photon [8,16] cavities to enhance the generation and detection mechanisms [17]. The theoretical framework was given by Thomsen et al. [1] and extended to multilayer samples by Matsuda and Wright [18].

In this paper we report on measurements in which a metal film and metal-dielectric superlattices are used for the excitation of phonon dynamics in the samples. By means of broadband optical light scattering we detect a broad spectrum of the excited phonon modes simultaneously. We show, how the detected phonons determine the oscillatory features in transient optical reflectivity measurements: near zero wavevector modes lead to oscillations that are visible in all probe wavelength equally while the detection of larger wavevector modes lead to an oscillation frequency dependent on probe wavelength. In particular we discuss how the spatial period of a superlattice determines which fraction of the Brillouin zone becomes observable by optical light scattering. We show measurements, in which the whole wavevector range of the superlattice Brillouin zone is observed.

2. Experiment

In phonon-light scattering experiments, the energy of phonons is much smaller than the energy of the probing photons leading to the approximation, that the absolute of the incident photon wavevector k is approximately equal to the absolute of the scattered photon wavevector k' : $k \approx k'$. Let us consider energy and momentum conservation, as illustrated in Fig. 1(a). In the scattering event the momentum component of the photons perpendicular to the momentum of the phonon is unaltered. The parallel component $k\cos\theta$ is changed by addition (or subtraction) of the energy and momentum of a phonon. The energy and the parallel component

* Corresponding author at: Institut für Physik & Astronomie, Universität Potsdam, Karl-Liebknecht-Str. 24-25, 14476 Potsdam, Germany.
E-mail address: bargheer@uni-potsdam.de (M. Bargheer).
URL: http://www.udkm.physik.uni-potsdam.de (M. Bargheer).

http://dx.doi.org/10.1016/j.ultras.2014.08.023
0041-624X/

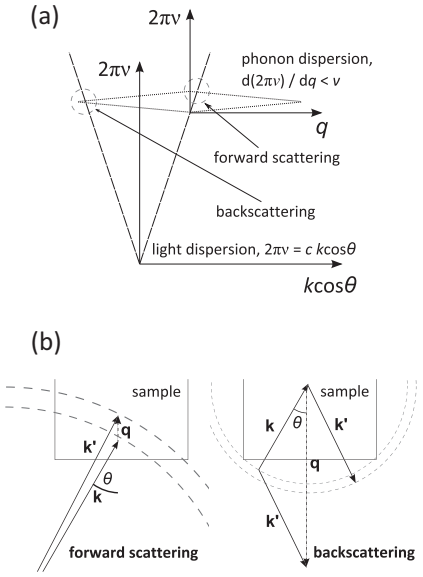

Fig. 1. (a) Illustration of energy and momentum conservation. A photon with given energy and momentum (dashed dispersion) can combine with a phonon (dotted dispersion, discussed in the next section) to form a new photon with approximately the same energy and momentum (forward scattering) or reversed momentum (backscattering). The energies are not drawn to scale, the light dispersion is much steeper in reality. (b) Illustration of momentum conservation and scattering geometry. In forward scattering the component of the incoming light parallel to the propagating phonon is nearly unaltered, in backscattering the component is reversed. The momenta are not drawn to scale. The changes in k and θ are not detectable in our experiment.

of the resulting photon must again fulfill the dispersion relation of light. Therefore, for a given photon there are two different solutions for the phonon involved (i. e. two intersection points in the figure) and thus two possible scattering regimes [19]. In the first regime the momentum of the scattering photon parallel to the travelling phonon is nearly unaltered (i.e. it is scattered in forward direction) and the transferred phonon momentum q is approximately zero:

$$q \approx 0 \quad \text{(forward scattering)} \tag{1}$$

The signature of this scattering regime is, that it occurs with approximately the same characteristic frequency for all photons independent of wavelength. It is usually detected in transmission geometry. We observe this type of scattering also in reflection geometry due to the reflection of the photons at different interfaces. In the second regime the momentum of the scattering photon parallel to the travelling phonon is reversed (i.e. it is scattered in backward direction) and the wavevector of the scattering phonon is thus given by:

$$q \approx 2k\cos\theta \quad \text{(backscattering)} \tag{2}$$

with internal angle of incidence with respect to the surface normal θ. Fig. 1(b) illustrates the vectorial nature of the momentum conservation for both scattering mechanisms: the photon momentum parallel to the phonon momentum is either reversed or nearly unchanged.

In time domain Brillouin scattering, the propagation of phonons that are coherently excited by a short pump pulse (excitation mechanism see below) are monitored by a delayed probe pulse. Instead of observing a spectral shift of the probe light as in ordinary (frequency domain) Brillouin scattering, we observe the frequency of the phonon in the time domain. Two effects modulate the light reflected from the sample by the frequency of the scattering phonons: one is, that the phonons present in the sample periodically modulate the optical properties of the different layers leading to a periodic modulation of the reflection from each interface (this is presumably the dominant effect in the multilayers, where the optical properties of the individual layers differ) and the other one is that the light field that undergoes Brillouin scattering from a phonon interferes with a static reference of the probe light reflected from the sample surface and interfaces. In this latter case the relative phase of the interfering signals varies with the phase of the scattering phonon or equivalently, the distance the lattice distortion has propagated into the sample and thus with the time delay between the pump and probe pulses, leading to constructive or destructive interference (this is the effect in the substrate).

The modulation frequency is simply given by $\nu(q \approx 0)$ for forward scattering and $\nu(q = 2k\cos\theta)$ for backscattering. For a linear phonon dispersion $2\pi\nu = v \cdot q$, with sound velocity v, follows for backscattering:

$$\nu = v \cdot 2k\cos\theta/(2\pi) = v \cdot 2n(\lambda)\cos\theta/\lambda \tag{3}$$

with vacuum probe wavelength λ and refractive index $n(\lambda)$.

In this paper we show measurements on phonon dynamics in three different samples (compare Table 1): (a) a 37 nm ($La_{0.7}Sr_{0.3}$)MnO_3 (LSMO) transducer film on a $SrTiO_3$ (STO) substrate, (b) an LSMO/($Ba_{0.7}Sr_{0.3}$)TiO_3 (BST) superlattice with 15 double layers of 21 nm period and (c) a $SrRuO_3$ (SRO)/STO superlattice with 5 double layers of 140 nm period. The samples were prepared using pulsed laser deposition [20]. Sketches of the samples are shown in the upper insets of Fig. 2.

We use optical pump pulses with 800 nm wavelength and 120 fs pulse duration derived from an amplified Ti–Sa laser system at a repetition rate of 5 kHz to excite the absorbing layers (LSMO and SRO) with a fluence of a few tens of mJ/cm^2. The rapid electron phonon coupling and subsequent thermal expansion of the metal layers launches strain pulses into the material. In the case of a single metal film (sample (a)) on a transparent substrate, a bipolar strain pulse [1] is generated and propagates into the substrate (compare Fig. 2(a), lower inset, finite laser penetration depth neglected). Exciting a superlattice (samples (b) and (c)), a pulse train is generated. In this case left and right propagating strain fronts start from each metal-dielectric interface and lead to an oscillatory movement of the layers (standing wave). These strain pulses eventually propagate into the substrate where they build a train of strain pulses [12] (compare Fig. 2(c), lower inset, finite laser penetration depth neglected). The propagation of the coherently generated phonon pulses is monitored by a delayed probe pulse, which scatters from these phonons. In order to simultaneously probe several phonon wavevectors we generate a white light continuum in a sapphire disc which is detected in reflection geometry using a fibre-optic spectrometer for broadband detection [11,21].

In Fig. 2 we show colour plots of the wavelength dependent transient optical reflectivity for the three different samples. An instantaneous electronic response and slow thermalization effects have been subtracted. Sample (a) shows oscillations described by Eq. (3). In this sample, the single LSMO layer expands and launches a bipolar strain pulse (as depicted in the lower inset of Fig. 2(a)) into the STO substrate underneath. Because of good acoustic matching between layer and substrate, the strain wave has

Table 1
Details of selected samples. Acronyms: interlayer (IL), amount of double layers (# DL), thin film (TF), superlattice (SL).

Nr.	Type	Metal	Dielectric IL	# DL	Substrate
(a)	TF	LSMO, 37 nm			STO (100)
(b)	SL	LSMO, 7.3 nm	BST, 13.7 nm	15	STO (100)
(c)	SL	SRO, 13 nm	STO, 127 nm	5	STO (100)